



HAL
open science

Low vulnerability of the Mediterranean antipatharian *Antipathella subpinnata* (Ellis & Solander, 1786) to ocean warming

Mathilde Godefroid, Tom Zeines, Lorenzo Bramanti, Pascal Romans, Marzia Bo, Margherita Toma, Bruno Danis, Philippe Dubois, Charlène Guillaumot

► **To cite this version:**

Mathilde Godefroid, Tom Zeines, Lorenzo Bramanti, Pascal Romans, Marzia Bo, et al.. Low vulnerability of the Mediterranean antipatharian *Antipathella subpinnata* (Ellis & Solander, 1786) to ocean warming. *Ecological Modelling*, 2023, 475, pp.110209. 10.1016/j.ecolmodel.2022.110209 . hal-03856980

HAL Id: hal-03856980

<https://hal.science/hal-03856980>

Submitted on 21 Nov 2022

HAL is a multi-disciplinary open access archive for the deposit and dissemination of scientific research documents, whether they are published or not. The documents may come from teaching and research institutions in France or abroad, or from public or private research centers.

L'archive ouverte pluridisciplinaire **HAL**, est destinée au dépôt et à la diffusion de documents scientifiques de niveau recherche, publiés ou non, émanant des établissements d'enseignement et de recherche français ou étrangers, des laboratoires publics ou privés.



Distributed under a Creative Commons Attribution - NonCommercial - NoDerivatives 4.0
International License

1 **Low vulnerability of the Mediterranean antipatharian *Antipathella subpinnata* (Ellis & Solander,**
2 **1786) to ocean warming**

3

4 Godefroid Mathilde^{1*}, Zeimes Tom^{1*}, Bramanti Lorenzo², Romans Pascal³, Bo Marzia⁴, Toma
5 Margherita⁴, Danis Bruno¹, Dubois Philippe^{1,#}, Guillaumot Charlène^{1,5,#}

6 ^{*,#}these authors contributed equally

7

8 ¹Université Libre de Bruxelles, Laboratoire de biologie marine, Avenue F.D. Roosevelt 50, CP160/15,
9 1050 Bruxelles, Belgium

10 ²LECOB/CNRS-Sorbonne Université UMR 8222, Observatoire Océanologique de Banyuls-sur-Mer,
11 Avenue Pierre Fabre 1, 66650 Banyuls-sur-Mer, France

12 ³CNRS-Sorbonne Université UMR 8222, Observatoire Océanologique de Banyuls-sur-Mer, Avenue
13 Pierre Fabre 1, 66650 Banyuls-sur-Mer, France

14 ⁴Università degli Studi di Genova, Dipartimento Scienze della Terra, dell’Ambiente e della Vita, Corso
15 Europa 26, 16132 Genova, Italy

16 ⁵CNRS/UB/EPHE, UMR 6282 Biogéosciences, Université Bourgogne Franche-Comté, Boulevard
17 Gabriel 6, 21000 Dijon, France

18

19 **Corresponding author** : Mathilde Godefroid

20 godefroid.mathilde1@gmail.com

21 Av. F.D. Roosevelt, CP160/15, 1050 Bruxelles, Belgium

22

23

24 **Abstract**

25 Antipatharians (black corals) are major components of mesophotic ecosystems in the Mediterranean
26 Sea. The arborescent species *Antipathella subpinnata* has received particular attention as it is the most
27 abundant and forms dense forests harbouring high levels of biodiversity. This species is currently
28 categorized as “Near Threatened” in the IUCN Red List, due to increasing fishing pressure and bottom-
29 trawling activities. Yet, the effects of ocean warming have never been investigated for this species, nor
30 for any other antipatharians from temperate regions. Our study aimed at evaluating the effects of
31 increasing seawater temperatures on *A. subpinnata*, by combining predictive distribution modelling
32 with a physiological tolerance experiment. During the latter, we exposed *A. subpinnata* for 15 days to
33 different temperature conditions spanning the current seasonal range to forecasted temperatures for
34 2100, while measuring biological endpoints such as oxygen consumption rates and different signs of
35 stress (tissue necrosis, total antioxidant capacity). Unexpectedly, no stress was found at organism nor
36 cellular level (wide thermal breadth) suggesting low susceptibility of this species to mid-term
37 temperature increase. If the response to the 15-days heat stress is representative of the response to
38 longer-term warming, ocean warming is unlikely to affect *A. subpinnata*. The species distribution
39 model predicted the presence of *A. subpinnata* at depths that correspond to temperatures colder than
40 its maximum thermal tolerance (as determined by the physiology experiment). This suggests that the
41 presence of *A. subpinnata* at shallower depths is not limited by physiological constraints but by other
42 ecological factors including interspecific competition.

43

44 **Keywords:** Antipatharia, thermotolerance, mesophotic, Mediterranean Sea, physiology, niche
45 modelling

46

47

48 **1. Introduction**

49 Greenhouse gas emission since 1750 has committed the global ocean to future warming. While the
50 amplitude of warming remains to be determined by our current actions, increase in global ocean
51 temperature is already irreversible (IPCC, 2022). The Mediterranean Sea and associated ecosystems
52 represent no exception. From 1982 to 2019, Mediterranean Sea surface temperatures (SST) have
53 increased by 0.35°C per decade (Pastor et al., 2020) and, under business-as-usual emissions (RCP8.5),
54 models forecast a rise of SST (0-150m) of +2.07-3.71°C by the end of the century (Soto-Navarro et al.,
55 2020).

56 Increasing ocean temperature is inducing a wide range of effects on marine organisms, as temperature
57 is one of the most important environmental factors for the majority of marine organisms (Yao &
58 Somero, 2014). Among the observed effects, ocean warming has been showed to modify the
59 distribution of certain species, which use this strategy to move towards areas matching their
60 environmental preferenda (Jorda et al., 2020). Other strategies to cope with ocean warming may
61 involve acclimatization to the new environmental conditions (i.e., phenotypic plasticity) or genetic
62 adaptation. Thus, experimental studies addressing responses to environmental changes should be
63 performed using organisms from different habitats as they can be adapted to local conditions and this
64 may explain why some ecosystems are more sensitive to warming than others. For example, a small
65 increase in temperature can be enough to drive significant consequences in ecosystems characterised
66 by extremely stable temperature, such as in the Southern Ocean (Hogg et al., 2011). Benthic organisms,
67 such as those forming Marine Animal Forests (MAFs; sensu Rossi et al., 2017), may also be particularly
68 threatened by ocean warming due to their inability to move away from adverse environmental
69 conditions.

70 The concept of MAF was recently introduced to describe benthic communities formed by sessile
71 suspension feeders (i.e., ecosystem engineers such as corals, sponges or bryozoans) that form three-
72 dimensional structures, resembling terrestrial forests. These communities increase habitat

73 heterogeneity, providing food, shelter and reproductive facilities for a plethora of associated fauna
74 (Rossi et al., 2017). The development of underwater imagery (Remotely Operated Vehicles,
75 submersibles) and deep diving techniques in recent years contributed to uncover that antipatharians
76 can also form MAFs (i.e., black coral forests) throughout the world oceans (Terrana et al., 2020;
77 Wagner et al., 2012).

78 In the Mediterranean Sea, the branched antipatharian *Antipathella subpinnata* (Ellis & Solander, 1786)
79 was reported to be one of the most frequently observed species in the mesophotic zone (Bo et al.,
80 2008, 2018, 2019; Ingrassia & Di Bella, 2021). Forests of *A. subpinnata* have been described in the
81 Tyrrhenian Sea (Bo et al., 2009, 2014; Gravier, 1918), the Ligurian Sea (Bo et al., 2008), the Adriatic Sea
82 (Chimienti et al., 2020), the Sardinian coast (Cau et al., 2015) and the Sicily Channel (Deidun et al.,
83 2014). The role of *A. subpinnata* as habitat forming species was evidenced by the great diversity of
84 associated fauna (Bo et al., 2012, 2015a), including multiple species of conservation and commercial
85 interest (Bo et al., 2009; Chimienti et al., 2020). The main anthropogenic threats for antipatharians in
86 the Mediterranean Sea are fishing and bottom trawling (Bo et al., 2009, 2019; Chimienti et al., 2020),
87 which may have long-lasting effects considering the low growth rates of these species (Bo et al.,
88 2015a). For these reasons, antipatharians have been mentioned in multiple international agreements
89 such as in the Appendix II of the CITES (Convention on International Trade in Endangered Species of
90 Wild Fauna and Flora), the Annex II of a Barcelona Convention Protocol for the Specially Protected Area
91 of Mediterranean Interest and the Annex III of the Berna Convention. Since 2014, *A. subpinnata* is
92 categorized as “Near Threatened” by the International Union for Conservation of Nature (IUCN) Red
93 List of Mediterranean Anthozoa (Bo et al., 2015b, 2017).

94 It is today acknowledged that ectotherms may be particularly sensitive to ocean warming as
95 temperature has direct effects on their biological processes across all levels of organization (Pörtner
96 and Farrell, 2008). Moreover, previous studies on Mediterranean epibenthic suspension feeders
97 showed that increasing temperature may have deleterious impacts, both in experimental conditions

98 and *in situ*, including mass-mortality events (Arizmendi-Mejía et al., 2015; Bramanti et al., 2005;
99 Cerrano et al., 2000; Garrabou et al., 2009; Kružić et al., 2016; Kipson et al., 2012; Linares et al., 2013).
100 To date, only one experiment addressed the effects of thermal stress in an antipatharian species
101 (*Stichopathes sp.*; Godefroid et al., 2022). This mesophotic tropical species was experimentally exposed
102 to medium-term (16 days) heat stress (up to 4.5°C), and results highlighted metabolic depression,
103 impairment of healing capacities and activation of stress response mechanisms (i.e., tissue necrosis,
104 mucus production and antioxidant responses). In the Mediterranean Sea, the effects of increasing
105 temperature on antipatharian species have never been investigated, despite the fact that temperature
106 has been shown to significantly influence their distribution (Etnoyer et al., 2018; Wagner, 2015; Yesson
107 et al., 2017). Investigating the effects of ocean warming is particularly relevant for *A. subpinnata*
108 forests, whose vulnerability is increased by the low genetic connectivity between offshore and coastal
109 populations (Terzin et al., 2021). To date, we only know that the species is likely limited below an upper
110 thermal threshold of 15°C, based on its depth distribution (mainly between 65 and 200m; Bo et al.,
111 2008). However, physiological studies on the effects of ocean warming on this species are currently
112 lacking.

113 In this study, we investigated the effects of increasing seawater temperature on the mesophotic
114 antipatharian *A. subpinnata* from the Mediterranean Sea, by combining experimental and distribution
115 modelling approaches. First, the experimental study aimed at establishing the thermal performance
116 curve (TPC) for respiration of *A. subpinnata*, as well as the impact of temperature on stress response
117 variables (tissue necrosis, antioxidant capacity, mortality). TPC allows describing thermal sensitivity of
118 organisms by determining a thermal window of performance (i.e., thermal breadth, T_{br}), characterized
119 by the so-called optimal temperature (T_{opt}) at which the performance is maximal (P_{max}) and beyond
120 which it starts to decrease (Angilletta, 2009; Schulte et al., 2011). Large T_{br} is often good indicator of
121 low sensitivity to changes in temperature, while narrow T_{br} often indicates high susceptibility as only a
122 small increase in temperature may result in suboptimal conditions (Jurriaans & Hoogenboom, 2020).
123 Based on Godefroid et al. (2022), we hypothesized that *A. subpinnata* has a narrow thermal window

124 and might be severely impacted by increasing temperatures. Then, we developed a Species
125 Distribution Model (SDM) to explore the role of temperature in the distribution of *A. subpinnata*. SDMs
126 are based on a statistical relationship between occurrence records and environmental data (Elith et
127 al., 2006; Elith & Leathwick, 2009), which are both available for *A. subpinnata* in the Mediterranean
128 Sea. Here, we used environmental conditions at the location of available presence-only data to
129 generate a matrix to build the SDM. The output represents the probability distribution of *A. subpinnata*
130 occurrence projected on a map, allowing to identify regions in the Mediterranean Sea where the
131 environment fulfils the required conditions. We also aimed at generating partial dependence plots for
132 each environmental descriptors used in the model, to assess if temperature is one of the main
133 environmental drivers for the distribution of *A. subpinnata* (as in Guillaumot et al., 2018). The
134 combination of the two approaches used in this study (physiological experiment + SDM) allowed to
135 improve predictions accuracy with respect to an approach based on the sole SDMs, as well as to
136 facilitate interpretation and infer robust conclusions (Benito Garzón et al., 2019; Buckley et al., 2010,
137 2011; Dormann et al., 2018; Elith et al., 2010; López-Farrán et al., 2021; Singer et al., 2016).

138

139 **2. Materials and Methods**

140 **2.1 Thermotolerance experiment**

141 2.1.1 Experimental design

142 Portions of seven adult colonies of *A. subpinnata* were collected by SCUBA diving (Self-Contained
143 Underwater Breathing Apparatus) with closed circuit rebreather at 70m depth in Bordighera (43°46.11'
144 N, 7°40.82' E, Ligurian sea, Italy) on March 29th 2021 (Fig. 1A). Seawater temperature at the time and
145 depth of collection was 14.5°C. During the collection, all the portions of the same colony were sealed
146 in the same plastic bag with seawater from the collection site. Seven plastic bags, containing portions
147 of seven coral colonies, were transported to Banyuls-sur-Mer aquarium facilities (*Biodiversarium*,
148 France) and portions of colonies were suspended in an open-circuit 2000-L tank filled with 0.2mm-

149 filtered seawater pumped at 12m depth and maintained, for 49 days, at 14.5°C using a water chiller
150 (AQUAVIE ICE-2000). After this acclimation period, six apical fragments (8-10 cm) were cut from each
151 colony, fixed on a PVC base using epoxy resin (Aquarium Systems, Holdfast epoxy) and installed in six
152 experimental aquaria (17 L) at 14.5°C (TECO; Fig. 1B). Each aquarium contained one fragment from
153 each colony ($n=7$). Fragments were left one week at 14.5°C and then temperature was progressively
154 decreased/increased by 0.5°C/day until reaching the target temperature. Treatment temperatures
155 were selected to span over the seasonal range of temperatures (13-16°C; Soto-Navarro et al., 2020) as
156 well as to include temperatures expected by the end of the century under Representative
157 Concentration Pathway (RCP) 8.5: 14, 15, 16, 17, 18 and 19°C. The six aquaria were placed in a
158 circulating water bath at 13°C which temperature was controlled using a water chiller (Teco; Fig. 1B).
159 In addition, temperature was controlled independently in each aquarium using temperature
160 controllers (Hobby Biotherm Pro) connected to a titanium heating resistance. Temperature was
161 manually checked at least twice per day with a thermometer (Ebro TFX-410-1). Filtered seawater (12m
162 depth, 0.2 mm diameter) was continuously flowing in each aquarium at a rate of 1.2 ± 0.3 L/hour. The
163 room was equipped with blue lights to simulate the natural light regime ($0.5 \mu\text{mol m}^{-2} \text{s}^{-1}$; photoperiod:
164 12h/day and 12h/night; based on Coppari et al., 2020). Colonies were fed once a day with live *Artemia*
165 *salina* and Rotifera provided by the aquarium facilities of *Biodiversarium*.

166 Outflows of seawater from each aquarium was equipped with a propagule trap composed of a 0.2 mm
167 net to catch bailed-out propagules. The formation of motile propagules from individual polyps was
168 proposed as an ultimate escape strategy in response to stressful conditions. It was previously observed
169 on *A. subpinnata* (Coppari et al., 2020) but never as a response to increasing temperatures. Every
170 morning, traps were checked for the presence of propagules under a dissecting microscope. Nets were
171 then cleaned before being placed back in the propagule traps.

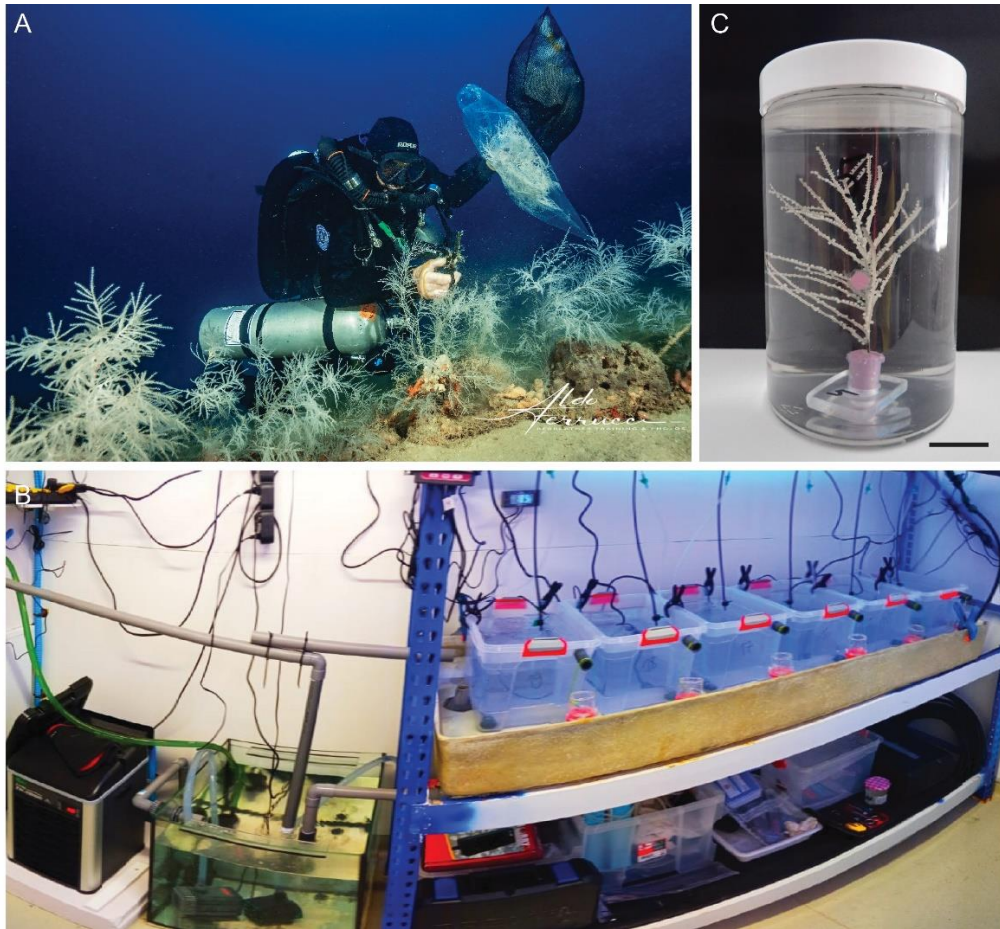
172 Tissue necrosis (i.e., the partial loss of live tissues around the skeleton) was recorded daily for all
173 fragments, as an estimated surface proportion (0, 25, 50, 75, 100%). Mortality (i.e., 100% tissue loss)
174 was also checked daily for all fragments and reported on a binary scale (dead/alive).

175 After 15 days of exposure, standard metabolic rate was inferred from oxygen consumption rates on
176 every fragment. Fragments were placed in individual 400-mL respirometry chambers filled with
177 seawater from the corresponding aquarium and provided with an oxygen sensor spot (PreSens SP-
178 PSt3-NAU-D5-YOP-SA) and a magnetic stir bar allowing complete homogenization of the water during
179 the measurement (Fig. 1C). Measurements of oxygen consumption were taken simultaneously on eight
180 respirometry chambers, with two respirometers (PreSens OXY-4 SMA G2 and OXY-4 SMA G3). One
181 chamber was only filled with seawater to measure the rate of background respiration (the respiration
182 of the microorganisms naturally present in seawater). The chambers were placed in a 60-L tank which
183 temperature was controlled with a heating resistance. First, chambers were left open for one hour in
184 the dark to allow the fragments to acclimatize to these conditions. Then, chambers were closed and
185 oxygen saturation (in %) was recorded every five seconds for three to four hours, using the Presens
186 Measurement Studio 2 software. Oxygen saturation measurements were normalized based on the
187 volume of seawater in the experimental chambers, calculated from the density of seawater (Millero &
188 Huang, 2009; Millero & Poisson, 1981). Oxygen saturation was then converted to oxygen concentration
189 (in $\mu\text{mol L}^{-1}$) and the rate of oxygen consumption was calculated from the slope of its linear regression
190 with time. Oxygen consumption rate of the fragments was corrected according to the consumption
191 rate of the seawater-only chamber and normalized by the total length of the fragment (i.e., sum of
192 length of all branches and branchlets) measured using ImageJ (Schneider et al., 2012). Oxygen
193 consumption rates were expressed in $\mu\text{mol O}_2 \text{ hr}^{-1} \text{ cm}^{-1}$ and in $\mu\text{mol O}_2 \text{ hour}^{-1} \text{ g}^{-1}$ (Fig. S4).

194 At the end of the respirometry assay, a 2-3 cm piece was cut from each coral fragment and placed in a
195 tube with phosphate buffer (50 mM), for biomarker analysis. Tissues were separated from the skeleton
196 and homogenized using a micro pestle. Homogenates were centrifuged for 10 min at 4°C (10000g,

197 Eppendorf Centrifuge 5430R) and the supernatant was transferred into a new tube and stored at -80°C
198 until analysis. The subsequent protocol was identical to that reported in Godefroid et al. (2022). Total
199 protein content in the samples was determined using a commercial reagent kit based on the Bradford
200 assay (Pierce™ BCA Protein Assay Kit, ThermoFisher Scientific Inc., USA) with bovine serum albumin
201 (BSA) as standard (2 mg/mL). Protein contents were used for biomarker normalization. Measurement
202 of total antioxidant capacity (TAC) was carried out using OxiSelect™ Total Antioxidant Capacity Assay
203 Kit (Cell Biolabs Inc., USA), an electron-transfer based assay (Huang et al., 2005) that measures the
204 capacity of an antioxidant solution to reduce an oxidant (Copper (II) reduced into Copper (I)). The
205 chromatic change is proportional with the sample antioxidant concentration. Absorbance was
206 measured at 490 nm in a microplate reader (Beckman Coulter Paradigm) and compared to uric acid
207 standard curves. Results were normalized to the protein content and expressed as “mM Copper
208 Reducing Equivalent per g of protein”.

209



210

211 **Figure 1.** (A) Collection of portions of colonies of *Antipathella subpinnata* at 70m in Bordighera (Italy). Photo credit: Aldo
 212 Ferrucci ; (B) Experimental set-up with the 6 aquaria, in the aquarium facilities of the *Biodiversarium*. Photo credit: Lorenzo
 213 Bramanti; (C) respirometry chamber containing a fragment of *Antipathella subpinnata*. Scale bar: 2cm. Photo credit: Tom
 214 Zeimes.

215

216 2.1.2 Data analysis

217 The relationship between respiration rate and temperature was analysed using a symmetrical Gaussian
 218 function (Rodolfo-Metalpa et al., 2014) fitted by non-linear regression with the R package *nlstools* (Baty
 219 et al., 2015):

220

$$P = P_{\max} e^{0.5 \left(\frac{T - T_{\text{opt}}}{c} \right)^2}$$

221 where P is the temperature dependent physiological response, T_{opt} is the optimal temperature at which
222 this response is maximal (P_{max}) and c indicates the breadth of the thermal response. The standard error
223 of the parameters estimates was also obtained with the model. The effect of temperature on TAC was
224 analysed using simple linear regression, with temperature as the independent variable.

225

226 **2.2 Species distribution modelling**

227

228 2.2.1 Occurrence dataset

229 Georeferenced presence-only data of *A. subpinnata* in the Mediterranean Sea were retrieved from the
230 archives of the *Università di Genova* ($n=85$) (Bo & Toma, unpublished data), the scientific literature
231 ($n=34$) (Bo et al., 2008, 2009, 2012, 2014; Canovas-Molinas et al., 2016; Cau et al., 2015, 2017;
232 Chimienti et al., 2020; Coppari et al., 2019; Fabri et al., 2014, 2019, 2021; Gaino & Scoccia, 2010;
233 Pierdomenico et al., 2016; Santin et al., 2021; van de Water et al., 2020), and the open-source GBIF
234 (Global Biodiversity Information Facility, $n=10$; Fautin, 2013; Orrell et al., 2022; iNaturalist, 2022;
235 Inventaire National du Patrimoine Naturel, 2022a, 2022b) and OBIS (Ocean Biodiversity Information
236 System, $n=2$; Hellenic Centre for Marine Research, 2022) databases. Some historical records were not
237 considered because they were lacking a systematic description (doubtful taxonomic determination)
238 and/or because coordinates were not available for the collected specimen (Bo et al., 2008). The dataset
239 was checked for redundant information (duplicates), georeferencing errors and inconsistencies. The
240 final dataset used for the distribution model included 131 presence-only records (Fig. S1). Absence
241 records were not taken into account.

242

243 2.2.2 Environmental data sets

244 The distribution of *A. subpinnata* was modelled using eight environmental descriptors (Table 1). Depth
 245 and slope were retrieved from the MARSPEC database (Sbrocco & Barber, 2013). The other six
 246 environmental descriptors were loaded from Bio-Oracle marine layers (Assis et al., 2018; Tyberghein
 247 et al., 2012).

248 All environmental layers were cropped to cover the same geographic area (Latitude: 28.60°N to
 249 47.60°N, Longitude: 5.75°W to 38.25°E). In order to limit extrapolation of the model, projection area
 250 was limited to habitats presenting a maximum depth of 1500m (Guillaumot et al., 2020a, 2021).

251 In order to identify and remove collinearity (i.e., the non-independence of predictor variables that are
 252 linearly related in a statistical model; Dormann et al., 2013) between environmental descriptors, the
 253 Variance Inflation Factor (VIF) and the Spearman correlation index were used (Guillaumot et al., 2019).

254 The VIF was calculated based on the equation:

$$255 \quad VIF_i = \frac{1}{R_i^2}$$

256 where R_i^2 is the determination coefficient of the prediction of all other variables (Dormann et al.,
 257 2013).

258

259 **Table 1.** Environmental descriptors and associated sources used for the distribution model. The Bio-ORACLE
 260 (<https://www.bio-oracle.org/>) environmental layers provide average monthly values for the period 2000-2014 at a
 261 spatial resolution of 0.083° and MARSPEC (<https://www.marspec.org/>) provides data layers at a spatial resolution of
 262 0.0083°. ORAP: Global Ocean Physics Reanalysis ECMWF; ARMOR: Global Observed Ocean Physics Reprocessing; PISCES:
 263 Global Ocean Biogeochemistry Non-assimilative Hindcast.

Descriptor	Unit	Spatial resolution	Source	Layers metadata
Depth	m	0.086°	MARSPEC	Extracted from SRTM30_PLUS V6.0 dataset (Becker et al., 2009; Sbrocco & Paul, 2013)
Slope	degrees (°)	0.086°	MARSPEC	Derived from bathymetry using ArcGIS 9.3.1; (Sbrocco & Paul, 2013)
Mean seafloor current	m.s ⁻¹	0.086°	Bio-ORACLE	ORAP (Assis et al., 2017)

Mean seafloor temperature	°C	0.086°	Bio-ORACLE	ARMOR (Assis et al., 2017)
Minimum seafloor temperature	°C	0.086°	Bio-ORACLE	ARMOR (Assis et al., 2017)
Maximal seafloor temperature	°C	0.086°	Bio-ORACLE	ARMOR (Assis et al., 2017)
Mean seafloor oxygen concentration	μmol.L ⁻¹	0.086°	Bio-ORACLE	PISCES (Assis et al., 2017)
Mean sea surface chlorophyll- <i>a</i> concentration	mg.m ⁻³	0.086°	Bio-ORACLE	PISCES (Assis et al., 2017)

264

265

266

2.2.3 Spatial aggregation: evaluation and correction

267

The distribution map of *A. subpinnata* in the Mediterranean Sea shows spatial heterogeneity in the

268

occurrence data, with more georeferenced data in the Tyrrhenian and Ligurian Seas (Fig. S1). Spatial

269

aggregation may result in overestimating the contribution of environmental variables in the most

270

densely sampled areas (Araújo & Guisan, 2006; Dormann, 2007). To correct the effect of spatial

271

aggregation of the presence-only data on modelling performance, we used a targeted sampling of

272

background data samples (Phillips et al., 2009). Background data are used in SDM having only

273

presence-only records to characterize the environmental conditions reported in the area where the

274

model will be projected (Barbet-Massin et al., 2012; Elith et al., 2006; Pearce & Boyce, 2006). Here, the

275

background data were sampled following the scheme of a Kernel Density Estimation layer (KDE) that

276

gives an estimate of the aggregation bias (Guillaumot et al., 2019). The KDE was calculated using the

277

function *kde2d* of the R package *MASS* (Fig. S2; Ripley, 2015). The significance of spatial aggregation of

278

presence data was quantified before and after the KDE correction, using the Moran's I index, that

279

evaluates the correlation between presence data and the probability of predicted presence based on

280

model residuals (Luoto et al., 2005). Moran's I values vary between -1 and 1, with positive values (0 to

281

1) reflecting that spatially close residuals will share similar presence probability and negative values (-

282

1 to 0) indicating a maximal or random dispersion of residuals in space (Cliff & Ord, 1981). This was

283

calculated using the R package *ape* (Paradis et al., 2019) for 15 model replicates.

284

285 2.2.4 Model calibration

286 SDMs were built using the Boosted Regression Trees (BRTs) algorithm, which were calibrated based on
287 the method provided in Elith et al. (2008). BRTs were selected as they were shown to be well-suited to
288 accommodate presence-only data and to integrate complex interactions between environmental
289 descriptors (Elith et al., 2008). Moreover, BRTs were shown to be suitable for oceanic datasets with
290 spatially autocorrelated and broad-scale presence-only datasets (Guillaumot et al., 2019). BRTs were
291 also shown to identify and delete redundant environmental information, therefore minimizing the
292 effect of collinearity of environmental descriptors (Guillaumot et al., 2020b). To calibrate the models,
293 the following settings were used: tree complexity 4; bag fraction 0.8; learning rate 0.011; and number
294 of background data sampled 10000. These parameters were chosen to minimise the model predictive
295 deviance to the test data (reduction of error) and to optimize the model with the minimum number of
296 trees (reduction of complexity) (Fig. S3).

297

298 2.2.5 Spatial cross-validation and model performances

299 Modelling performance was assessed using a spatial random cross-validation procedure, as in
300 Guillaumot et al. (2019). Considering the spatial aggregation of occurrence records in the dataset, the
301 occurrence dataset was randomly split into four spatial groups, using the function *get.block* from the
302 R package *ENMeval* (Kass et al., 2021). Three out of four groups were used as a training subset and one
303 group as a test subset. When the proportion of correct predictions in the test group was above 70%,
304 the pixel was considered as favourable for *A. subpinnata*. Model performance was also assessed using
305 the area under the curve (AUC; Fielding & Bell, 1997), the true skill statistics (TSS; Allouche et al., 2006)
306 and the biserial correlation metrics (COR; Elith et al., 2006).

307

308 2.2.6 Spatial extrapolation

309 The Multivariate Environmental Similarity Surface (MESS) index (Elith et al., 2010) was used to remove
310 extrapolation errors in the model, using the R function *mess* in the package *dismo* (Hijmans et al.,
311 2017). It consists in extracting the environmental conditions where presence data were recorded and
312 determining for each pixel of the model projection layer if environmental conditions are covered by
313 presence record (Guillaumot et al., 2019). It allows to dismiss areas where environmental conditions
314 are not met, when the value of at least one environmental descriptor is beyond the environmental
315 range of presence records (model extrapolation; negative MESS values).

316

317 2.2.7 Model outputs

318 In total, 50 SDMs with distinct background samplings were generated with the R function *compute.brt*
319 of the package *SDMPlay* (Guillaumot et al., 2021). The average of the 50 replicates was used to build
320 the SDM projections of the presence probability. *SDMPlay* was also used to assess the contribution of
321 each environmental descriptors to the model, i.e. the importance of each descriptor in the model
322 calibration.

323

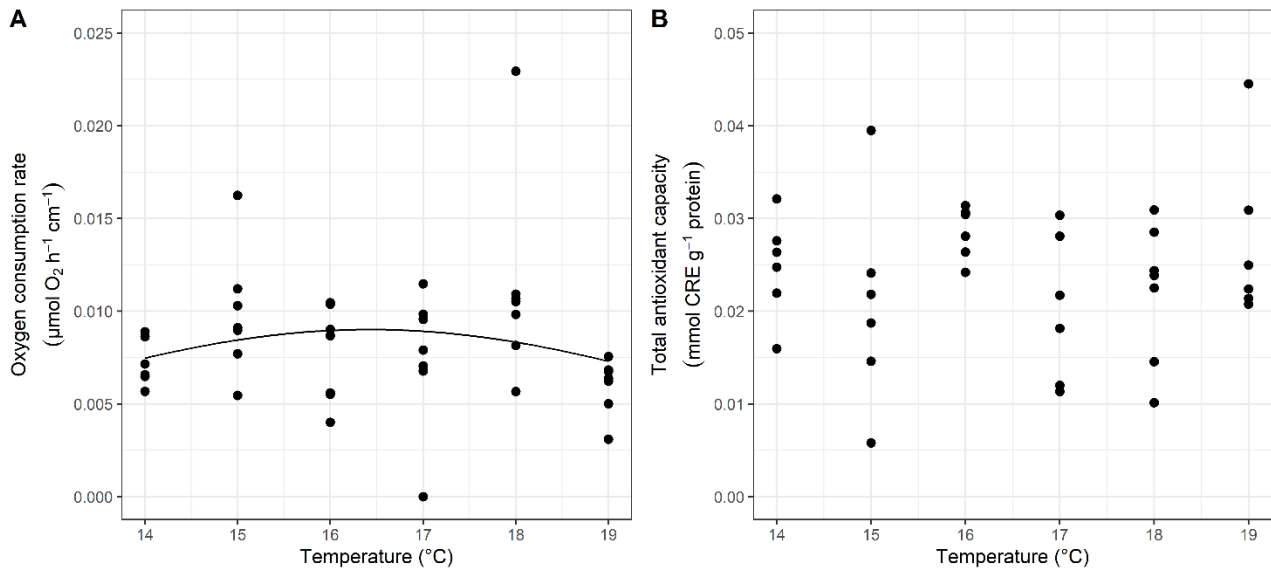
324 3. Results

325 3.1 Thermotolerance experiment

326 Neither tissue necrosis, mortality nor polyp bail-out were observed in any treatment over the course
327 of the experiment. The relationship between oxygen consumption rate and temperature can be
328 described by a Gaussian curve (Fig. 2A) with its maximum ($0.009 \pm 0.001 \mu\text{mol O}_2 \text{ h}^{-1} \text{ cm}^{-2}$; mean \pm se;
329 $p < 0.001$; P_{max}) at $16.4 \pm 0.7^\circ\text{C}$ ($p < 0.001$; T_{opt}). The standard deviation of the curve (c) was estimated in
330 $4.0 \pm 1.7^\circ\text{C}$ ($p < 0.05$). Similar results were obtained when oxygen consumption was normalized using

331 the weight of the fragments (Fig. S4, Table S1). Finally, temperature had no significant effect on the
332 antioxidant capacity of *A. subpinnata* (linear regression, $p=0.76$; Fig. 2B).

333



334

335 **Figure 2.** Effects of temperature on *Antipathella subpinnata* (A) Oxygen consumption rate (µmol O₂ h⁻¹ cm⁻¹), (B) Total
336 antioxidant capacity (mmol Copper Reducing Equivalent g⁻¹ protein).

337

338 3.2 SDM projections under current environmental conditions (2000-2014)

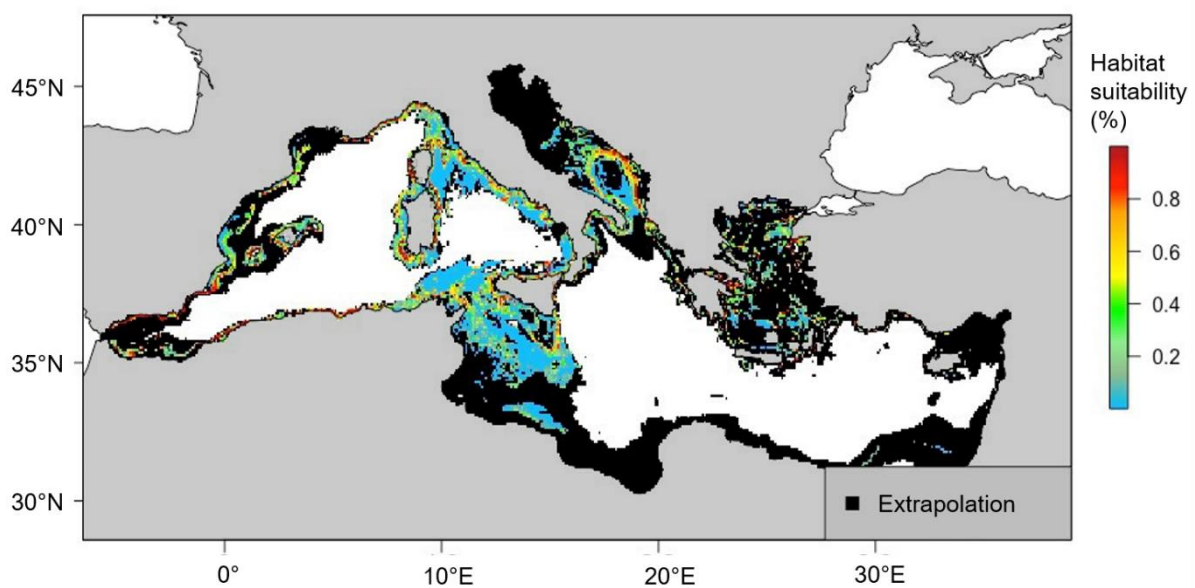
339 SDMs showed high performance scores, with AUC of 0.999 ± 0.001 , TSS of 0.738 ± 0.017 and COR of
340 0.972 ± 0.007 . The proportion of correctly classified test data also showed high values for the four
341 groups of occurrence data used for spatial cross-validation, with $98.42 \pm 2.49\%$ (mean \pm se) for group
342 1, $98.19 \pm 2.81\%$ for group 2, $99.60 \pm 1.47\%$ for group 3 and $96.69 \pm 4.04\%$ for group 4. The proportion
343 of extrapolated area was 65.86% (Fig. 3), supporting the use of the MESS method (Guillaumot et al.,
344 2019, 2020a).

345 In addition to the occurrence data of *A. subpinnata* in the Tyrrhenian, Ligurian, Adriatic, Ionian and
346 Aegean Seas (Fig. S1), the model projected very high presence probabilities in the Alboran Sea (South
347 coast of Spain and North coast of Morocco), along the Algerian coast, around the Balearic Islands, along

348 the East coast of the Adriatic Sea (Coasts of Croatia, Bosnia and Herzegovina, Montenegro, Albania)
349 and in the South coast of Greece, near Athens (Fig. 3). Model projections also suggested an
350 intermediate probability of presence in the Balearic and Adriatic Seas, around Corsica, Sardinia, Sicily
351 and Malta, and in the waters between the coast of Tunisia and Sicily (Fig. 3).

352

353



354

355 **Figure 3.** Distribution model predictions of the likelihood of presence of *Antipathella subpinnata* (between 0 and 1) under
356 current environmental conditions (2000-2014) for the Mediterranean Sea. Model results are the average of 50 model
357 replicates. Black pixels indicate areas of model extrapolation, where environmental conditions are outside the conditions
358 used for their calibration (i.e., Multivariate Environmental Similarity Surface, MESS index evaluation). White pixels correspond
359 to areas of the Mediterranean Sea that are deeper than 1,500m.

360

361 The two main descriptors contributing to the species distribution model are slope ($45.9 \pm 13.2\%$) and
362 depth ($43.9 \pm 13.6\%$), which together contributed to 89.8% (Table 2). In contrast, environmental
363 descriptors characterizing seafloor temperature only contributed for 5.4%, including $2.4 \pm 0.8\%$ for
364 minimum, $1.7 \pm 0.8\%$ for maximum and $1.3 \pm 0.6\%$ for mean seafloor temperatures. Suitable areas for

365 depth were found in the range of 60 to 325m, with a maximum occurrence probability at 240m.
 366 Occurrence probability as predicted by the model remained high between 325 and 600m depth but
 367 were unlikely below 600m (Fig. 4). Suitable habitats for temperature corresponded to mean
 368 temperatures between 14.3 and 15.9°C (with a predicted maximum at 14.9°C), maximum
 369 temperatures between 14.7 and 18°C (with a predicted maximum at 15.2°C) (Fig. 4). Despite its major
 370 contribution to the model, partial dependence plot for the slope did not allow identifying clear
 371 environmental preferences for this descriptor (Fig. 4).

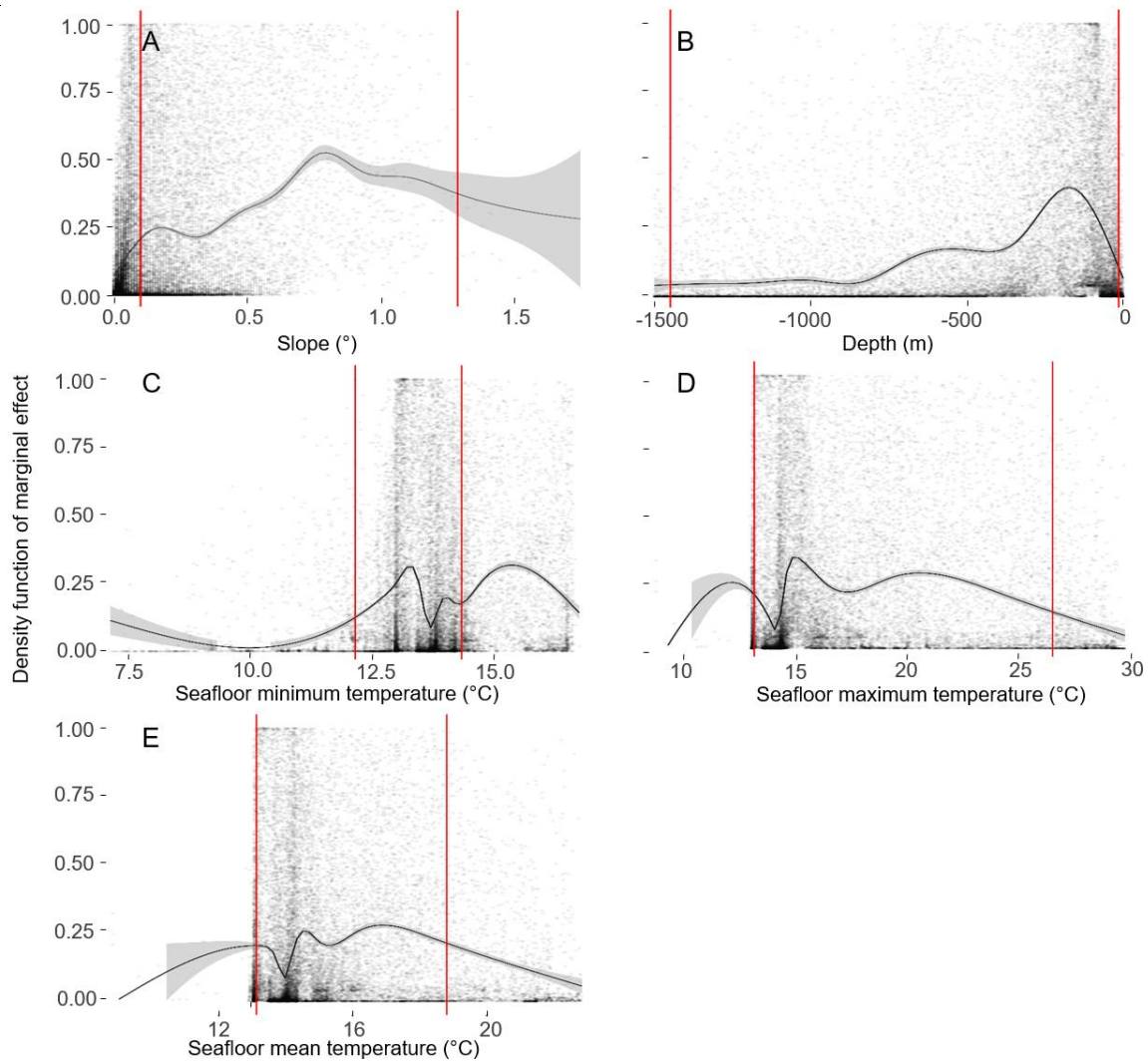
372

373 **Table 2.** Environmental descriptors contributions (mean and standard deviation - SD)
 374 to model calibration

375

Environmental descriptor	Mean ± SD (%)
Slope	45.9 ± 13.2
Depth	43.9 ± 13.6
Minimum seafloor temperature	2.4 ± 0.8
Mean sea surface chlorophyll- <i>a</i> concentration	1.9 ± 0.7
Maximum seafloor temperature	1.7 ± 0.8
Mean seafloor current	1.6 ± 0.6
Mean seafloor oxygen	1.4 ± 0.4
Mean seafloor temperature	1.3 ± 0.6

376



377

378 **Figure 4.** Partial dependence plots for the two descriptors that contributed the most to the model: Slope (A) and Depth (B);
 379 and for the environmental descriptors associated to seafloor temperature: Minimum (C), Maximum (D) and Mean (E). Data
 380 points (black) were fitted with General Additive Model (GAM, black line). Vertical red lines indicate the range of values in
 381 which the model does not extrapolate.

382

383 4. Discussion

384 Spatial ecology and experimental biology have long been considered as separate research disciplines.
 385 Yet, a number of studies have shown that combining both approaches can improve species distribution
 386 projections in the context of ongoing climate change (Kotta et al., 2019; Urban et al., 2016). In order
 387 to achieve more robust projections of biotic patterns, information gathered from physiological

388 tolerance experiments should also be incorporated (Buckley et al., 2010). For these reasons, we
389 combined experimental and modelling approaches to investigate the effects of increasing
390 temperatures on the branched antipatharian *A. subpinnata* from the Mediterranean Sea. Results from
391 spatial predictive modelling indicated that the distribution of *A. subpinnata* is driven by a combination
392 of interacting factors rather than by a single leading environmental descriptor. For depth, the upper
393 and lower bathymetric limits estimated by the model at 60 and 600m respectively, match with
394 observations from Bo et al. (2008). Ocean current is also important for antipatharians as it provides
395 them with suspended food particles (Genin et al., 1986; Warner, 1981). However, hydrodynamic
396 preferences vary between species. The unbranched species from Indonesia were shown to
397 preferentially select sites with higher hydrodynamics than branched species (Tazioli et al., 2007), as
398 further supported by higher bending resistance in unbranched species (Dugauquier et al., 2021). This
399 may explain the preferences of *A. subpinnata* to relatively gentle slopes and moderate current speeds.
400 For temperature, mean temperature correlating with its distribution ranged between 14.3 and 15.9°C
401 (with a maximum at 14.9°C) and the upper limit of the range of maximum temperature was 18°C,
402 suggesting that *A. subpinnata* can thrive at 18°C for several days. Such a narrow temperature interval
403 may either indicate that the species is not physiologically able to survive at temperatures outside this
404 range, or that other factors involved in the areas where temperatures are not in this range prevent the
405 establishment of *A. subpinnata*. SDM projections also highlighted the areas with favourable
406 environmental conditions for *A. subpinnata* but where no occurrences have been recorded to date in
407 the Mediterranean Sea. These model outputs could help guide future exploration and sampling efforts
408 as well as providing further validation of the model. In addition, some areas in the Mediterranean Sea
409 where high probability of presence were identified by the model to coincide with areas of some of the
410 historical taxonomic determinations that could not be used in the presence data to build the model as
411 they were doubtful and/or lacked georeferencing data (Bo et al., 2008). Examples include specimens
412 near Gibraltar (Alboran Sea; Ellis & Solander, 1786) and along the Algerian coast (Vafidis & Koukouras;
413 1998). This provides additional data supporting the model.

414 Results obtained from the thermotolerance experiment suggest that *A. subpinnata* will not be
415 impacted by temperature expected by the end of the century (19°C, +4.5°C), at the studied time scale
416 (15 days). No signs of stress were detected, without mortality, tissue necrosis nor effects on the
417 antioxidant response at any temperature, while a previous experiment on the tropical antipatharian
418 *Stichopathes* sp. recorded tissue necrosis under only +3°C for 16 days (Godefroid et al., 2022). High
419 tissue necrosis was also noticed in the temperate coral *Cladocora caespitosa* subjected to +3°C for 3
420 weeks, followed by subsequent mortality (Kersting et al., 2013; Rodolfo-Metalpa et al., 2005). In
421 addition, bail-out propagules were never found in the traps, which may indicate that these
422 temperature conditions were not stressful for *A. subpinnata* or that temperature do not trigger the
423 formation of propagules. Indeed, the stress factor responsible for the release of free-living propagules
424 in *A. subpinnata* has not yet been identified (Coppari et al., 2020). Despite this, active detachment of
425 polyps from the colony under warmer conditions was previously observed for the tropical scleractinian
426 *Pocillopora damicornis* (Fordyce et al., 2017), supporting the idea that temperature projected for 2100
427 is not high enough to trigger this response in *A. subpinnata*. This is further supported by the absence
428 of antioxidant response. If increasing temperature had created oxidative stress at cellular level, the
429 organism would have used antioxidant defence mechanisms to counter these effects. Such response
430 was previously observed in the antipatharian *Stichopathes* sp. (+4.5°C for 16 days; Godefroid et al.,
431 2022) and in tropical corals (+4°C for 60 days; Dias et al., 2019).

432 The effects of temperature on oxygen consumption rates allowed to identify an optimal temperature
433 (T_{opt}) at 16.4°C, beyond which metabolic rate starts to decrease with temperature. This is likely related
434 to the disruption of enzymatic activities with increasing temperature, rather than by a reduction of
435 metabolic costs (Jurriaans & Hoogenboom, 2020). However, the width of the thermal window of
436 performance (T_{br}) was large (6°C) as compared to a similar thermotolerance experiment on the tropical
437 antipatharian *Stichopathes* sp. (with T_{br} of 3.2°C; Godefroid et al., 2022), suggesting that increasing
438 temperature is likely to have less impact on *A. subpinnata*. A wide T_{br} is often described as a good

439 strategy in front of ocean warming as it implies that an increase in temperature will have milder effects
440 on performances as compared to species with narrow T_{br} (Jurriaans & Hoogenboom, 2020).

441 Overall, physiological results suggest that *A. subpinnata* is not strongly influenced by temperature and
442 is likely a thermal generalist species with low thermal sensitivity. This strategy is characterized by the
443 ability of the species to maintain the integrity of their physiological functions over a wide range of
444 temperatures (Angiletta, 2009). However, SDMs showed that the distribution of *A. subpinnata* is more
445 likely between mean temperatures of 14.3-15.9°C, which is below T_{opt} (16.4°C). Ideally, *A. subpinnata*
446 should be present in habitats which temperature is close to T_{opt} , to optimize its metabolic activity.
447 However, this inconsistency should be weighed by the wide thermal breadth (T_{br}) of *A. subpinnata*
448 (6°C) which covers the entire range of mean temperatures predicted by the model. That is, even if *A.*
449 *subpinnata* lives in suboptimal conditions in terms of metabolic performances, the drop in
450 performance remains low owing to its wide T_{br} .

451 A possible explanation for the mismatch between T_{opt} and suitable average temperatures for *A.*
452 *subpinnata* calculated by the SDM may be biotic interactions such as interspecific competition. SDMs
453 are built based on presence-only data and allow to represent the realized niche of a species (i.e., the
454 area in which the species is found), constrained by biotic factors, abiotic conditions and the regions
455 that are accessible to dispersal by the species (Soberon & Peterson, 2005). However, SDMs are limited
456 by their incapacity to explicitly integrate biotic interactions in model construction (Saucède et al.,
457 2019).

458 In tropical reef ecosystems, community structure is characterized by depth zonation caused by
459 multiple factors such as competitive interactions or light. Shallow waters are dominated by obligatory
460 photosynthetic organisms such as algae and corals, while deep waters are mainly composed of
461 facultatively or non-photosynthetic organisms (Kahng & Kelley, 2007; Wagner et al., 2012).
462 Temperature and light gradient are key intercorrelated factors in regulating the distribution of species
463 across depths (Kahng & Kelley, 2007). Suitable habitats and bathymetric distribution of antipatharians

464 are thus the result of abiotic and biotic interactions (Tazioli et al., 2007; Wagner et al., 2012). In tropical
465 shallow habitats, antipatharians compete for space with zooxanthellate scleractinians (Tazioli et al.,
466 2007) and macrophytes (Kahng & Kelley, 2007). Larvae or bailed-out propagules' settlement could be
467 inhibited by the mechanical action of the macrophytes sweeping the substrate. In case of successful
468 settlement, they would probably be outcompeted by surrounding macrophytes and scleractinians
469 which are characterized by faster growth rates. We suggest that the competition for space with
470 crustose coralline algae and other habitat-forming species (sponges and Anthozoans) may also explain
471 the distribution of *A. subpinnata* in the Mediterranean Sea. The actual distribution of *A. subpinnata*
472 would therefore not be the consequence of physiological limitations, as suggested by Bo et al. (2008),
473 but rather the result of interspecific competition and probably also larval dispersal (completely
474 unknown for this species).

475 As a consequence of global warming, mean shallow-water temperature (0-150m) in the Mediterranean
476 is expected to increase by 3.7°C under the most pessimistic scenario (RCP 8.5; Soto-Navarro et al.,
477 2020). Even under this extreme scenario, seawater temperature will remain within the large thermal
478 tolerance window of *A. subpinnata*, suggesting that it should not suffer from deleterious physiological
479 impacts, if results obtained here over short-term (15 days) also apply to longer term. How thermal
480 tolerance estimated under experimental conditions can be extrapolated to natural settings is an
481 ongoing debate. It is noteworthy that the duration and intensity of the experimental assay influence
482 the observed response (Sinclair et al., 2016). For example, the mechanisms influencing performance
483 at acute and chronic time scales may be quite different, and TPC shape can change with acclimation
484 (Schulte et al., 2011). Rezende et al (2014) demonstrated that the temperature range that an organism
485 can tolerate is expected to narrow down with the duration of the thermal challenge. With this in mind,
486 it could be that we did not observe any effects over 15d but would have if exposure had been longer
487 (>15d). Despite this, none of the endpoints recorded during the experiment seem to indicate a sign of
488 stress, neither at the physiological, nor at the subcellular level (antioxidant response). In addition, the
489 capacity for plastic responses to changing temperatures can also depend on the rate of temperature

490 change, and generally, organisms that are shifted slowly to higher temperatures are expected to
491 perform better than those that are exposed to fast warming rate (*e.g.* Sobek et al. 2011). Here,
492 warming rate from the acclimatisation to the test temperature was faster than the warming rate
493 expected under OW. The observed responses therefore potentially worsen the effects, compared to a
494 more gradual (realistic) temperature increase. For all these reasons, we do not see any obvious reason
495 to doubt the high tolerance of *A. subpinnata* under OW.

496

497 **Acknowledgements**

498 We would like to thank Davide Mottola and the Nautilus Technical Diving for colonies collection, Aldo
499 Ferrucci for taking pictures during sampling, the team of aquariologists from the *Biodiversarium* for
500 their advice and help in setting up the aquarium, the platform BIO2MAR (with special thanks to Drs N.
501 West and L. Intertaglia) for the access to the microplate reader and J. Boeuf for her help during our
502 stay at OOB.

503

504 **Funding**

505 The research leading to these results received funding from the European Union's Horizon 2020
506 research and innovation programme [grant number 730984], the ASSEMBLE Plus project and the FNRS
507 project COBICO [grant number T0084.18]. M. Godefroid is holder of a Belgian FRIA grant [FRS-FNRS,
508 number 1.E.066.19F]. Ph. Dubois is a research director of the National Fund for Scientific Research
509 (FRS-FNRS; Belgium).

510

511

512

513 **CRedit (Contribution Roles Taxonomy) author statement**

514 **Godefroid Mathilde:** Conceptualization, Methodology, Software, Formal analysis, Investigation,
515 Writing – Original draft, Visualization, Funding acquisition; **Zeimes Tom:** Conceptualization,
516 Methodology, Software, Formal analysis, Investigation, Writing – Review & Editing; **Bramanti Lorenzo:**
517 Resources, Supervision, Writing – Review & Editing, Funding acquisition; **Romans Pascal:** Resources,
518 Writing – Review & Editing; **Bo Marzia:** Resources, Writing – Review & Editing; **Toma Margherita:**
519 Resources, Writing – Review & Editing; **Danis Bruno:** Writing – Review & Editing; **Dubois Philippe:**
520 Conceptualization, Methodology, Writing – Review & Editing, Supervision, Funding acquisition;
521 **Guillaumot Charlène:** Conceptualization, Methodology, Software, Formal analysis, Writing – Review &
522 Editing.

523

524

525 **References**

- 526 Allouche, O., Tsoar, A., & Kadmon, R. (2006). Assessing the accuracy of species distribution models:
527 Prevalence, kappa and the true skill statistic (TSS): Assessing the accuracy of distribution
528 models. *Journal of Applied Ecology*, 43(6), 1223–1232. [https://doi.org/10.1111/j.1365-](https://doi.org/10.1111/j.1365-2664.2006.01214.x)
529 [2664.2006.01214.x](https://doi.org/10.1111/j.1365-2664.2006.01214.x)
- 530 Angilletta, M. J. (2009). *Thermal adaptation: A theoretical and empirical synthesis*. Oxford University
531 Press.
- 532 Araújo, M. B., & Guisan, A. (2006). Five (or so) challenges for species distribution modelling. *Journal*
533 *of Biogeography*, 33(10), 1677–1688. <https://doi.org/10.1111/j.1365-2699.2006.01584.x>
- 534 Arizmendi-Mejía, R., Ledoux, J. B., Civit, S., Antunes, A., Thanopoulou, Z., Garrabou, J., & Linares, C.
535 (2015). Demographic responses to warming: reproductive maturity and sex influence
536 vulnerability in an octocoral. *Coral Reefs*, 34(4), 1207–1216.
- 537 Assis, J., Tyberghein, L., Bosch, S., Verbruggen, H., Serrão, E. A., De Clerck, O., & Tittensor, D. (2018).
538 Bio-ORACLE v2.0: Extending marine data layers for bioclimatic modelling. *Global Ecology and*
539 *Biogeography*, 27(3), 277–284. <https://doi.org/10.1111/geb.12693>
- 540 Barbet-Massin, M., Jiguet, F., Albert, C. H., & Thuiller, W. (2012). Selecting pseudo-absences for
541 species distribution models: How, where and how many?: *How to use pseudo-absences in*
542 *niche modelling? Methods in Ecology and Evolution*, 3(2), 327–338.
543 <https://doi.org/10.1111/j.2041-210X.2011.00172.x>
- 544 Baty F, Ritz C, Charles S, Brutsche M, Flandrois J-P, Delignette-Muller M-L (2015). A Toolbox for
545 Nonlinear Regression in R: The Package nlstools. *Journal of Statistical Software*, 66(5), 1-21.
546 <https://doi.org/10.18637/jss.v066.i05>
- 547 Becker, J. J., D. T. Sandwell, W. H. F. Smith, J. Braud, B. Binder, J. Depner, D. Fabre, J. Factor, S. Ingalls,
548 S-H. Kim, R. Ladner, K. Marks, S. Nelson, A. Pharaoh, R. Trimmer, J. Von Rosenberg, G.
549 Wallace, and P. Weatherall. 2009. Global Bathymetry and Elevation Data at 30 Arc Seconds
550 Resolution: SRTM30_PLUS. *Marine Geodesy* 32:355–371.
551 <https://doi.org/10.1080/01490410903297766>
- 552 Benito Garzón, M., Robson, T. M., & Hampe, A. (2019). Δ Trait SDMs: Species distribution models that
553 account for local adaptation and phenotypic plasticity. *New Phytologist*, 222(4), 1757–1765.
554 <https://doi.org/10.1111/nph.15716>
- 555 Bo, M., Barucca, M., Biscotti, M. A., Brugler, M. R., Canapa, A., Canese, S., Lo Iacono, C., &
556 Bavestrello, G. (2018). Phylogenetic relationships of Mediterranean black corals (Cnidaria:

557 Anthozoa : Hexacorallia) and implications for classification within the order Antipatharia.
558 *Invertebrate Systematics*, 32(5), 1102. <https://doi.org/10.1071/IS17043>

559 Bo, M., Bavestrello, G., Angiolillo, M., Calcagnile, L., Canese, S., Cannas, R., Cau, A., D'Elia, M.,
560 D'Oriano, F., Follesa, M. C., Quarta, G., & Cau, A. (2015a). Persistence of Pristine Deep-Sea
561 Coral Gardens in the Mediterranean Sea (SW Sardinia). *PLOS ONE*, 10(3), e0119393.
562 <https://doi.org/10.1371/journal.pone.0119393>

563 Bo, M., Orejas, C., Garcia, S., Antoniadou, C. & Cerrano, C. (2015b). *Antipathella subpinnata*. *The*
564 *IUCN Red List of Threatened Species* 2015: e.T50902681A50902879. Accessed on 10 February
565 2022.

566 Bo, M., Bavestrello, G., Canese, S., Giusti, M., Salvati, E., Angiolillo, M., & Greco, S. (2009).
567 Characteristics of a black coral meadow in the twilight zone of the central Mediterranean
568 Sea. *Marine Ecology Progress Series*, 397, 53–61. <https://doi.org/10.3354/meps08185>

569 Bo, M., Canese, S., & Bavestrello, G. (2014). Discovering Mediterranean black coral forests:
570 *Parantipathes larix* (Anthozoa: Hexacorallia) in the Tuscan Archipelago, Italy. *Italian Journal of*
571 *Zoology*, 81(1), 112–125. <https://doi.org/10.1080/11250003.2013.859750>

572 Bo, M., Canese, S., Spaggiari, C., Pusceddu, A., Bertolino, M., Angiolillo, M., Giusti, M., Loreto, M. F.,
573 Salvati, E., Greco, S., & Bavestrello, G. (2012). Deep Coral Oases in the South Tyrrhenian Sea.
574 *PLoS ONE*, 7(11), e49870. <https://doi.org/10.1371/journal.pone.0049870>

575 Bo, M., Montgomery, A. D., Opresko, D. M., Wagner, D., & Bavestrello, G. (2019). Antipatharians of
576 the Mesophotic Zone: Four Case Studies. In Y. Loya, K. A. Puglise, & T. C. L. Bridge (Eds.),
577 *Mesophotic Coral Ecosystems* (Vol. 12, pp. 683–708). Springer International Publishing.
578 https://doi.org/10.1007/978-3-319-92735-0_37

579 Bo, M., Numa, C., del Mar Otero, M., Orejas, C., Garrabou, J., Cerrano, C., Kružić, P., Antoniadou, C.,
580 Aguilar, R., Kipson, S., Linares, C., Terrón-Sigler, A., Brossard, J., Kersting, D., Casado-Amezúa,
581 P., García, S., Goffredo, S., Ocaña, O., Caroselli, E., ... Özalp, B. (2017). *Overview of the*
582 *conservation status of Mediterranean anthozoa*. IUCN International Union for Conservation
583 of Nature. <https://doi.org/10.2305/IUCN.CH.2017.RA.2.en>

584 Bo, M., Tazioli, S., Spanò, N., & Bavestrello, G. (2008). *Antipathella subpinnata* (Antipatharia,
585 Myriopathidae) in Italian seas. *Italian Journal of Zoology*, 75(2), 185–195.
586 <https://doi.org/10.1080/11250000701882908>

587 Buckley, L. B., Urban, M. C., Angilletta, M. J., Crozier, L. G., Rissler, L. J., & Sears, M. W. (2010). Can
588 mechanism inform species' distribution models?: Correlative and mechanistic range models.
589 *Ecology Letters*, no-no. <https://doi.org/10.1111/j.1461-0248.2010.01479.x>

590 Buckley, L. B., Waaser, S. A., MacLean, H. J., & Fox, R. (2011). Does including physiology improve
591 species distribution model predictions of responses to recent climate change? *Ecology*,
592 92(12), 2214–2221. <https://doi.org/10.1890/11-0066.1>

593 Cánovas-Molina, A., Montefalcone, M., Bavestrello, G., Cau, A., Bianchi, C. N., Morri, C., ... & Bo, M.
594 (2016). A new ecological index for the status of mesophotic megabenthic assemblages in the
595 Mediterranean based on ROV photography and video footage. *Continental Shelf*
596 *Research*, 121, 13-20. <https://doi.org/10.1016/j.csr.2016.01.008>

597 Cau, A., Follesa, M. C., Moccia, D., Alvito, A., Bo, M., Angiolillo, M., Canese, S., Paliaga, E. M., Orrù, P.
598 E., Sacco, F., & Cannas, R. (2015). Deepwater corals biodiversity along roche du large
599 ecosystems with different habitat complexity along the south Sardinia continental margin
600 (CW Mediterranean Sea). *Marine Biology*, 162(9), 1865–1878.
601 <https://doi.org/10.1007/s00227-015-2718-5>

602 Cau, A., Moccia, D., Follesa, M. C., Alvito, A., Canese, S., Angiolillo, M., Cuccu, D., Bo, M., & Cannas, R.
603 (2017). Coral forests diversity in the outer shelf of the south Sardinian continental margin.
604 *Deep Sea Research Part I: Oceanographic Research Papers*, 122, 60–70.
605 <https://doi.org/10.1016/j.dsr.2017.01.016>

606 Cerrano, C., Bavestrello, G., Bianchi, C. N., Cattaneo-vietti, R., Bava, S., Morganti, C., Morri, C., Picco,
607 P., Sara, G., Schiaparelli, S., Siccardi, A., & Sponga, F. (2000). A catastrophic mass-mortality
608 episode of gorgonians and other organisms in the Ligurian Sea (North-western
609 Mediterranean), summer 1999. *Ecology Letters*, 3(4), 284–293.
610 <https://doi.org/10.1046/j.1461-0248.2000.00152.x>

611 Chimienti, G., De Padova, D., Mossa, M., & Mastrototaro, F. (2020). A mesophotic black coral forest
612 in the Adriatic Sea. *Scientific Reports*, 10(1). <https://doi.org/10.1038/s41598-020-65266-9>

613 Cliff, A. & Ord, J.K. (1981). *Spatial Processes Models and Applications*. Pion Ltd.

614 Coppari, M., Fumarola, L., Bramanti, L., Romans, P., Pillot, R., Bavestrello, G., & Bo, M. (2020).
615 Unveiling asexual reproductive traits in black corals: Polyp bail-out in *Antipathella*
616 *subpinnata*. *Coral Reefs*. <https://doi.org/10.1007/s00338-020-02018-1>

617 Coppari, M., Mestice, F., Betti, F., Bavestrello, G., Castellano, L., & Bo, M. (2019). Fragmentation, re-
618 attachment ability and growth rate of the Mediterranean black coral *Antipathella*
619 *subpinnata*. *Coral Reefs*, 38(1), 1–14. <https://doi.org/10.1007/s00338-018-01764-7>

620 Deidun, A., Andaloro, F., Bavestrello, G., Canese, S., Consoli, P., Micallef, A., Romeo, T., & Bo, M.
621 (2014). First characterisation of a *Leiopathes glaberrima* (Cnidaria: Anthozoa: Antipatharia)
622 forest in Maltese exploited fishing grounds. *Italian Journal of Zoology*, 1–10.
623 <https://doi.org/10.1080/11250003.2014.986544>

624 Dias, M., Madeira, C., Jogee, N., Ferreira, A., Gouveia, R., Cabral, H., Diniz, M., & Vinagre, C. (2019).
625 Oxidative stress on scleractinian coral fragments following exposure to high temperature and
626 low salinity. *Ecological Indicators*, *107*, 105586.
627 <https://doi.org/10.1016/j.ecolind.2019.105586>

628 Dormann, C. F. (2007). Effects of incorporating spatial autocorrelation into the analysis of species
629 distribution data. *Global Ecology and Biogeography*, *16*(2), 129–138.
630 <https://doi.org/10.1111/j.1466-8238.2006.00279.x>

631 Dormann, C. F., Bobrowski, M., Dehling, D. M., Harris, D. J., Hartig, F., Lischke, H., Moretti, M. D.,
632 Pagel, J., Pinkert, S., Schleuning, M., Schmidt, S. I., Sheppard, C. S., Steinbauer, M. J., Zeuss,
633 D., & Kraan, C. (2018). Biotic interactions in species distribution modelling: 10 questions to
634 guide interpretation and avoid false conclusions. *Global Ecology and Biogeography*, *27*(9),
635 1004–1016. <https://doi.org/10.1111/geb.12759>

636 Dormann, C. F., Elith, J., Bacher, S., Buchmann, C., Carl, G., Carré, G., Marquéz, J. R. G., Gruber, B.,
637 Lafourcade, B., Leitão, P. J., Münkemüller, T., McClean, C., Osborne, P. E., Reineking, B.,
638 Schröder, B., Skidmore, A. K., Zurell, D., & Lautenbach, S. (2013). Collinearity: A review of
639 methods to deal with it and a simulation study evaluating their performance. *Ecography*,
640 *36*(1), 27–46. <https://doi.org/10.1111/j.1600-0587.2012.07348.x>

641 Dugauquier, J., Godefroid, M., M'Zoudi, S., Terrana, L., Todinanahary, G., Eeckhaut, I., & Dubois, P.
642 (2021). Ecomechanics of black corals (Cnidaria: Anthozoa: Hexacorallia: Antipatharia): A
643 comparative approach. *Invertebrate Biology*. <https://doi.org/10.1111/ivb.12347>

644 Elith, J., H. Graham, C., P. Anderson, R., Dudík, M., Ferrier, S., Guisan, A., J. Hijmans, R., Huettmann,
645 F., R. Leathwick, J., Lehmann, A., Li, J., G. Lohmann, L., A. Loiselle, B., Manion, G., Moritz, C.,
646 Nakamura, M., Nakazawa, Y., McC. M. Overton, J., Townsend Peterson, A., ... E.
647 Zimmermann, N. (2006). Novel methods improve prediction of species' distributions from
648 occurrence data. *Ecography*, *29*(2), 129–151. [https://doi.org/10.1111/j.2006.0906-](https://doi.org/10.1111/j.2006.0906-7590.04596.x)
649 [7590.04596.x](https://doi.org/10.1111/j.2006.0906-7590.04596.x)

650 Elith, J., Kearney, M., & Phillips, S. (2010). The art of modelling range-shifting species: *The art of*
651 *modelling range-shifting species*. *Methods in Ecology and Evolution*, *1*(4), 330–342.
652 <https://doi.org/10.1111/j.2041-210X.2010.00036.x>

653 Elith, J., & Leathwick, J. R. (2009). Species Distribution Models: Ecological Explanation and Prediction
654 Across Space and Time. *Annual Review of Ecology, Evolution, and Systematics*, *40*(1), 677–
655 697. <https://doi.org/10.1146/annurev.ecolsys.110308.120159>

656 Elith, J., Leathwick, J. R., & Hastie, T. (2008). A working guide to boosted regression trees. *Journal of*
657 *Animal Ecology*, *77*(4), 802–813. <https://doi.org/10.1111/j.1365-2656.2008.01390.x>

658 Ellis, J. & Solander, D. (1786). The Natural History of many curious and uncommon Zoophytes,
659 collected from various parts of the Globe. Systematically arranged and described by the late
660 Daniel Solander. 4. (Benjamin White & Son: London): 1-206, pls 1-63., *available online*
661 *at* <https://www.biodiversitylibrary.org/page/41943909>

662 Etnoyer, P. J., Wagner, D., Fowle, H. A., Poti, M., Kinlan, B., Georgian, S. E., & Cordes, E. E. (2018).
663 Models of habitat suitability, size, and age-class structure for the deep-sea black coral
664 *Leiopathes glaberrima* in the Gulf of Mexico. *Deep Sea Research Part II: Topical Studies in*
665 *Oceanography*, 150, 218–228. <https://doi.org/10.1016/j.dsr2.2017.10.008>

666 Fabri, M.-C., Pedel, L., Beuck, L., Galgani, F., Hebbeln, D., & Freiwald, A. (2014). Megafauna of
667 vulnerable marine ecosystems in French mediterranean submarine canyons: Spatial
668 distribution and anthropogenic impacts. *Deep Sea Research Part II: Topical Studies in*
669 *Oceanography*, 104, 184–207. <https://doi.org/10.1016/j.dsr2.2013.06.016>

670 Fabri Marie-Claire (2021). Antipatharians (Hexacorallia) presence and absence data reported from
671 canyons along the french mediterranean coast (2009-2010).
672 Ifremer. <https://doi.org/10.12770/1d1e0bdd-f72e-461b-8294-5f0c0c17239c>

673 Fabri, M.-C., Vinha, B., Allais, A.-G., Bouhier, M.-E., Dugornay, O., Gaillot, A., & Arnaubec, A. (2019).
674 Evaluating the ecological status of cold-water coral habitats using non-invasive methods: An
675 example from Cassidaigne canyon, northwestern Mediterranean Sea. *Progress in*
676 *Oceanography*, 178, 102172. <https://doi.org/10.1016/j.pocean.2019.102172>

677 Fautin, Daphne G. (2013). Hexacorallians of the World. <https://doi.org/10.15468/90drpi> accessed via
678 GBIF.org on 2022-06-09. <https://www.gbif.org/occurrence/2520740051>

679 Fielding, A. H., & Bell, J. F. (1997). A review of methods for the assessment of prediction errors in
680 conservation presence/absence models. *Environmental Conservation*, 24(1), 38–49.
681 <https://doi.org/10.1017/S0376892997000088>

682 Fordyce, A. J., Camp, E. F., & Ainsworth, T. D. (2017). *Table of qualitative observations of polyp*
683 *bailout in control and heat-treated mesocosms*. [Data set]. F1000Research.
684 <https://doi.org/10.5256/F1000RESEARCH.11522.D161213>

685 Gaino, E., & Scoccia, F. (2010). Gamete spawning in *Antipathella subpinnata* (Anthozoa,
686 Antipatharia): A structural and ultrastructural investigation. *Zoomorphology*, 129(4), 213–
687 219. <https://doi.org/10.1007/s00435-010-0112-x>

688 Garrabou, J., Coma, R., Bensoussan, N., Bally, M., Chevaldonné, P., Cigliano, M., ... & Cerrano, C.
689 (2009). Mass mortality in Northwestern Mediterranean rocky benthic communities: effects of
690 the 2003 heat wave. *Global change biology*, 15(5), 1090-1103. [https://doi-](https://doi-org.ezproxy.ulb.ac.be/10.1111/j.1365-2486.2008.01823.x)
691 [org.ezproxy.ulb.ac.be/10.1111/j.1365-2486.2008.01823.x](https://doi-org.ezproxy.ulb.ac.be/10.1111/j.1365-2486.2008.01823.x)

692

693 Genin, A., Dayton, P. K., Lonsdale, P. F., & Spiess, F. N. (1986). Corals on seamount peaks provide
694 evidence of current acceleration over deep-sea topography. *Nature*, 322(6074), 59–61.
695 <https://doi.org/10.1038/322059a0>

696 Godefroid, M., Hédouin, L., Mercière, A., & Dubois, P. (2022). Thermal stress responses of the
697 antipatharian *Stichopathes* sp. From the mesophotic reef of Mo'orea, French Polynesia.
698 *Science of The Total Environment*, 820, 153094.
699 <https://doi.org/10.1016/j.scitotenv.2022.153094>

700 Gravier, C. Notes on the Antipatharians of the Gulf of Naples. (1918). *Pubblicazioni della Stazione*
701 *Zoologica di Napoli* 2, 223–240.

702 Guillaumot, C., Artois, J., Saucède, T., Demoustier, L., Moreau, C., Eléaume, M., Agüera, A., & Danis,
703 B. (2019). Broad-scale species distribution models applied to data-poor areas. *Progress in*
704 *Oceanography*, 175, 198–207. <https://doi.org/10.1016/j.pocean.2019.04.007>

705 Guillaumot, C., Fabri-Ruiz, S., Martin, A., Eléaume, M., Danis, B., Féral, J.-P., & Saucède, T. (2018).
706 Benthic species of the Kerguelen Plateau show contrasting distribution shifts in response to
707 environmental changes. *Ecology and Evolution*, 8(12), 6210–6225.
708 <https://doi.org/10.1002/ece3.4091>

709 Guillaumot, C., Moreau, C., Danis, B., & Saucède, T. (2020a). Extrapolation in species distribution
710 modelling. Application to Southern Ocean marine species. *Progress in Oceanography*, 188,
711 102438. <https://doi.org/10.1016/j.pocean.2020.102438>

712 Guillaumot, C., Danis, B. & Saucède, T. (2020b). Selecting environmental descriptors is critical for
713 modelling the distribution of Antarctic benthic species. *Polar Biology*, 43(9), 1363–1381.
714 <https://doi.org/10.1007/s00300-020-02714-2>

715 Guillaumot, C., Martin, A., Eleaume, M., & Saucède, T. (2021). SDMPlay : Species Distribution
716 Modelling Playground. <https://CRAN.R-project.org/package=SDMPlay>

717 Hellenic Centre for Marine Research, MedOBIS - Mediterranean Ocean Biodiversity Information
718 System. (2022). Hellenic Centre for Marine Research; Institute of Marine Biology and Genetics;
719 Biodiversity and Ecosystem Management Department, Heraklion, Greece.
720 <http://ipt.vliz.be/eurobis/>

721 Hijmans, R.J., Phillips, S., Leathwick, J. & Elith, J. (2017). R package “dismo”.
722 <https://CRAN.Rproject.org/package=dismo>

723 Hogg, O. T., Barnes, D. K. A., & Griffiths, H. J. (2011). Highly Diverse, Poorly Studied and Uniquely
724 Threatened by Climate Change: An Assessment of Marine Biodiversity on South Georgia's
725 Continental Shelf. *PLoS ONE*, 6(5), e19795. <https://doi.org/10.1371/journal.pone.0019795>
726 iNaturalist contributors, iNaturalist (2022). iNaturalist Research-grade Observations. iNaturalist.org.
727 Occurrence dataset <https://doi.org/10.15468/ab3s5x> accessed via GBIF.org on 2022-06-09.

728 Ingrassia, M., & Di Bella, L. (2021). Black Coral Distribution in the Italian Seas: A Review. *Diversity*, 13(7),
729 334. <https://doi.org/10.3390/d13070334>

730 Inventaire National du Patrimoine Naturel N (2022a). Programme d'acquisition et de valorisation de
731 données naturalistes BioObs - Observations naturalistes des Amis de BioObs.. Version 1.1. UMS
732 PatriNat (OFB-CNRS-MNHN), Paris. Occurrence dataset <https://doi.org/10.15468/ldch7a>
733 accessed via GBIF.org on 2022-06-09. <https://www.gbif.org/occurrence/3472852485>

734 Inventaire National du Patrimoine Naturel N (2022b). Programme CARTHAM: Inventaire biologique
735 dans le cadre de Natura 2000 en Mer. Version 1.1. UMS PatriNat (OFB-CNRS-MNHN), Paris.
736 Occurrence dataset <https://doi.org/10.15468/3isrct> accessed via GBIF.org on 2022-06-09.
737 <https://www.gbif.org/occurrence/2488021119>

738 IPCC. (2022). Summary for Policymakers [H.-O. Pörtner, D.C. Roberts, E.S. Poloczanska, K.
739 Mintenbeck, M. Tignor, A. Alegría, M. Craig, S. Langsdorf, S. Löschke, V. Möller, A. Okem
740 (eds.)]. In: *Climate Change 2022: Impacts, Adaptation, and Vulnerability. Contribution of*
741 *Working Group II to the Sixth Assessment Report of the Intergovernmental Panel on Climate*
742 *Change* [H.-O. Pörtner, D.C. Roberts, M. Tignor, E.S. Poloczanska, K. Mintenbeck, A. Alegría,
743 M. Craig, S. Langsdorf, S. Löschke, V. Möller, A. Okem, B. Rama (eds.)]. Cambridge University
744 Press. In Press.

745 Jorda, G., Marbà, N., Bennett, S., Santana-Garcon, J., Agusti, S., & Duarte, C. M. (2020). Ocean
746 warming compresses the three-dimensional habitat of marine life. *Nature Ecology &*
747 *Evolution*, 4(1), 109–114. <https://doi.org/10.1038/s41559-019-1058-0>

748 Jurriaans, S., & Hoogenboom, M. (2020). Seasonal acclimation of thermal performance in two species
749 of reef-building corals. *Marine Ecology Progress Series*, 635, 55–70.
750 <https://doi.org/10.3354/meps13203>

751 Kahng, S. E., & Kelley, C. D. (2007). Vertical zonation of megabenthic taxa on a deep photosynthetic
752 reef (50–140 m) in the Au'au Channel, Hawaii. *Coral Reefs*, 26(3), 679–687.
753 <https://doi.org/10.1007/s00338-007-0253-7>

754 Kass, J. M., Muscarella, R., Galante, P. J., Bohl, C. L., Pinilla-Buitrago, G. E., Boria, R. A., Soley-Guardia,
755 M., & Anderson, R. P. (2021). ENMeval 2.0: Redesigned for customizable and reproducible

756 modeling of species' niches and distributions. *Methods in Ecology and Evolution*, 12(9),
757 1602–1608. <https://doi.org/10.1111/2041-210X.13628>

758 Kersting, D. K., Bensoussan, N., & Linares, C. (2013). Long-Term Responses of the Endemic Reef-
759 Builder *Cladocora caespitosa* to Mediterranean Warming. *PLoS ONE*, 8(8), e70820.
760 <https://doi.org/10.1371/journal.pone.0070820>

761 Kipson, S., Linares, C., Teixidó, N., Bakran-Petricioli, T., & Garrabou, J. (2012). Effects of thermal stress
762 on early developmental stages of a gorgonian coral. *Marine Ecology Progress Series*, 470, 69-
763 78. <https://doi.org/10.3354/meps09982>

764 Kotta, J., Vanhatalo, J., Jänes, H., Orav-Kotta, H., Rugiu, L., Jormalainen, V., Bobsien, I., Viitasalo, M.,
765 Virtanen, E., Sandman, A. N., Isaeus, M., Leidenberger, S., Jonsson, P. R., & Johannesson, K.
766 (2019). Integrating experimental and distribution data to predict future species patterns.
767 *Scientific Reports*, 9(1). <https://doi.org/10.1038/s41598-018-38416-3>

768 Kružić, P., Rodić, P., Popijač, A., & Sertić, M. (2016). Impacts of temperature anomalies on mortality
769 of benthic organisms in the Adriatic Sea. *Marine ecology*, 37(6), 1190-
770 1209. <https://doi.org/10.1111/maec.12293>

771 Linares, C., Cebrian, E., Kipson, S., & Garrabou, J. (2013). Does thermal history influence the tolerance
772 of temperate gorgonians to future warming?. *Marine environmental research*, 89, 45-52.
773 <https://doi.org/10.1016/j.marenvres.2013.04.009>

774 López-Farrán, Z., Guillaumot, C., Vargas-Chacoff, L., Paschke, K., Dulière, V., Danis, B., Poulin, E.,
775 Saucède, T., Waters, J., & Gérard, K. (2021). Is the southern crab *Halicarcinus planatus*
776 (Fabricius, 1775) the next invader of Antarctica? *Global Change Biology*, 27(15), 3487–3504.
777 <https://doi.org/10.1111/gcb.15674>

778 Luoto, M., Pöyry, J., Heikkinen, R. K., & Saarinen, K. (2005). Uncertainty of bioclimate envelope
779 models based on the geographical distribution of species: Uncertainty of bioclimate envelope
780 models. *Global Ecology and Biogeography*, 14(6), 575–584. <https://doi.org/10.1111/j.1466-822X.2005.00186.x>

782 Millero, F. J., & Huang, F. (2009). The density of seawater as a function of salinity (5 to 70 g kg^{−1})
783 and temperature (273.15 to 363.15 K). *Ocean Science*, 5(2), 91–100.
784 <https://doi.org/10.5194/os-5-91-2009>

785 Millero, F. J., & Poisson, A. (1981). International one-atmosphere equation of state of seawater. *Deep*
786 *Sea Research Part A. Oceanographic Research Papers*, 28(6), 625–629.
787 [https://doi.org/10.1016/0198-0149\(81\)90122-9](https://doi.org/10.1016/0198-0149(81)90122-9)

788 Orrell T, Informatics Office (2022). NMNH Material Samples (USNM). Version 1.41. National Museum
789 of Natural History, Smithsonian Institution. Occurrence dataset

790 <https://doi.org/10.15468/jb9tdf> accessed via GBIF.org on 2022-06-09.
791 <https://www.gbif.org/occurrence/3027965257>

792 Paradis, B. T., Henry, R. P., & Chadwick, N. E. (2019). Compound effects of thermal stress and tissue
793 abrasion on photosynthesis and respiration in the reef-building coral *Acropora cervicornis*
794 (Lamarck, 1816). *Journal of Experimental Marine Biology and Ecology*, *521*, 151222.
795 <https://doi.org/10.1016/j.jembe.2019.151222>

796 Pastor, F., Valiente, J. A., & Khodayar, S. (2020). A Warming Mediterranean: 38 Years of Increasing
797 Sea Surface Temperature. *Remote Sensing*, *12*(17), 2687.
798 <https://doi.org/10.3390/rs12172687>

799 Pearce, J. L., & Boyce, M. S. (2006). Modelling distribution and abundance with presence-only data.
800 *Journal of Applied Ecology*, *43*(3), 405–412. [https://doi.org/10.1111/j.1365-](https://doi.org/10.1111/j.1365-2664.2005.01112.x)
801 [2664.2005.01112.x](https://doi.org/10.1111/j.1365-2664.2005.01112.x)

802 Phillips, S. J., Dudík, M., Elith, J., Graham, C. H., Lehmann, A., Leathwick, J., & Ferrier, S. (2009).
803 Sample selection bias and presence-only distribution models: Implications for background
804 and pseudo-absence data. *Ecological Applications*, *19*(1), 181–197.
805 <https://doi.org/10.1890/07-2153.1>

806 Pierdomenico, M., Martorelli, E., Dominguez-Carrió, C., Gili, J. M., & Chiocci, F. L. (2016). Seafloor
807 characterization and benthic megafaunal distribution of an active submarine canyon and
808 surrounding sectors: The case of Gioia Canyon (Southern Tyrrhenian Sea). *Journal of Marine*
809 *Systems*, *157*, 101-117. <https://doi.org/10.1016/j.jmarsys.2016.01.005>

810 Pörtner, H. O., & Farrell, A. P. (2008). Physiology and climate change. *Science*, 690-692.

811 Ripley, B. (2015). MASS: Support Functions and Datasets for Venables and Ripley's MASS. 2015.
812 <https://CRAN.R-project.org/package=MASS>. R package version, pp. 7–3.

813 Rodolfo-Metalpa, R., Bianchi, C. N., Peirano, A., & Morri, C. (2005). Tissue necrosis and mortality of
814 the temperate coral *Cladocora Caespitosa*. *Italian Journal of Zoology*, *72*(4), 271–276.
815 <https://doi.org/10.1080/11250000509356685>

816 Rodolfo-Metalpa, R., Hoogenboom, M. O., Rottier, C., Ramos-Esplá, A., Baker, A. C., Fine, M., &
817 Ferrier-Pagès, C. (2014). Thermally tolerant corals have limited capacity to acclimatize to
818 future warming. *Global Change Biology*, *20*(10), 3036–3049.
819 <https://doi.org/10.1111/gcb.12571>

820 Rossi, S., Bramanti, L., Gori, A., Orejas, C. (2017). An Overview of the Animal Forests of the World. *In*
821 *book: Marine Animal Forests, pp.1-26. SPRINGER.[DOI: 10.1007/978-3-319-17001-5_1-1]*

822 Santin, A., Aguilar, R., Akyol, O., Begburs, C., Benoit, L., Chimienti, G., ... & Andreu, S. (2021). New
823 records of rare species in the Mediterranean Sea (March 2021). *Mediterranean Marine*
824 *Science*, 22(1), 199-217.

825 Saucède, T., Guillaumot, C., Michel, L. N., Fabri-Ruiz, S., Bazin, A., Cabessut, M., García-Berro, A.,
826 Mateos, A., Ridder, C. D., Dubois, P., Danis, B., David, B., Lepoint, G., Motreuil, S., Poulin, E.,
827 & Féral, J.-P. (2019). *Modelling species response to climate change in sub-Antarctic islands:*
828 *Echinoids as a case study for the Kerguelen Plateau*. 22.

829 Sbrocco, E., & Barber, P. (2013). MARSPEC: ocean climate layers for marine spatial ecology: Ecological
830 Archives E094-086. *Ecology*, 94(4), 979.

831 Schneider, C. A., Rasband, W. S., & Eliceiri, K. W. (2012). NIH Image to ImageJ: 25 years of image
832 analysis. *Nature Methods*, 9(7), 671–675. [doi:10.1038/nmeth.2089](https://doi.org/10.1038/nmeth.2089)

833 Schulte, P. M., Healy, T. M., & Fanguie, N. A. (2011). Thermal Performance Curves, Phenotypic
834 Plasticity, and the Time Scales of Temperature Exposure. *Integrative and Comparative*
835 *Biology*, 51(5), 691–702. <https://doi.org/10.1093/icb/icr097>

836 Singer, A., Johst, K., Banitz, T., Fowler, M. S., Groeneveld, J., Gutiérrez, A. G., Hartig, F., Krug, R. M.,
837 Liess, M., Matlack, G., Meyer, K. M., Pe'er, G., Radchuk, V., Voinopol-Sassu, A.-J., & Travis, J.
838 M. J. (2016). Community dynamics under environmental change: How can next generation
839 mechanistic models improve projections of species distributions? *Ecological Modelling*, 326,
840 63–74. <https://doi.org/10.1016/j.ecolmodel.2015.11.007>

841 Soberon, J., & Peterson, A. T. (2005). Interpretation of Models of Fundamental Ecological Niches and
842 Species' Distributional Areas. *Biodiversity Informatics*, 2(0).
843 <https://doi.org/10.17161/bi.v2i0.4>

844 Soto-Navarro, J., Jordá, G., Amores, A., Cabos, W., Somot, S., Sevault, F., Macías, D., Djurdjevic, V.,
845 Sannino, G., Li, L., & Sein, D. (2020). Evolution of Mediterranean Sea water properties under
846 climate change scenarios in the Med-CORDEX ensemble. *Climate Dynamics*, 54(3–4), 2135–
847 2165. <https://doi.org/10.1007/s00382-019-05105-4>

848 Tazioli, S., Bo, M., Boyer, M., Rotinsulu, H., & Bavestrello, G. (2007). Ecological Observations of Some
849 Common Antipatharian Corals in the Marine Park of Bunaken (North Sulawesi, Indonesia).
850 *Zoological Studies*, 15.

851 Terrana, L., Bo, M., Opresko, D. M., & Eeckhaut, I. (2020). Shallow-water black corals (Cnidaria:
852 Anthozoa: Hexacorallia: Antipatharia) from SW Madagascar. *Zootaxa*, 4826(1), 1–62.
853 <https://doi.org/10.11646/zootaxa.4826.1.1>

854 Terzin, M., Paletta, M. G., Matterson, K., Coppari, M., Bavestrello, G., Abbiati, M., Bo, M., &
855 Costantini, F. (2021). Population genomic structure of the black coral *Antipathella subpinnata*

856 in Mediterranean Vulnerable Marine Ecosystems. *Coral Reefs*, 40(3), 751–766.
857 <https://doi.org/10.1007/s00338-021-02078-x>

858 Tyberghein, L., Verbruggen, H., Pauly, K., Troupin, C., Mineur, F., & De Clerck, O. (2012). Bio-ORACLE:
859 A global environmental dataset for marine species distribution modelling: Bio-ORACLE
860 marine environmental data rasters. *Global Ecology and Biogeography*, 21(2), 272–281.
861 <https://doi.org/10.1111/j.1466-8238.2011.00656.x>

862 Urban, M. C., Bocedi, G., Hendry, A. P., Mihoub, J.-B., Pe'er, G., Singer, A., Bridle, J. R., Crozier, L. G.,
863 De Meester, L., Godsoe, W., Gonzalez, A., Hellmann, J. J., Holt, R. D., Huth, A., Johst, K., Krug,
864 C. B., Leadley, P. W., Palmer, S. C. F., Pantel, J. H., ... Travis, J. M. J. (2016). Improving the
865 forecast for biodiversity under climate change. *Science*, 353(6304).
866 <https://doi.org/10.1126/science.aad8466>

867 Vafidis D, Koukouras A. (1998). Antipatharia, Ceriantharia and Zoantharia (Hexacorallia, Anthozoa) of
868 the Aegean Sea with a check list of the Mediterranean and Black Sea Species. *Annales de*
869 *l'Institut océanographique*, Paris 74:115–126.

870 van de Water, J. A. J. M., Coppari, M., Enrichetti, F., Ferrier-Pagès, C., & Bo, M. (2020). Local
871 Conditions Influence the Prokaryotic Communities Associated With the Mesophotic Black
872 Coral *Antipathella subpinnata*. *Frontiers in Microbiology*, 11.
873 <https://doi.org/10.3389/fmicb.2020.537813>

874 Wagner, D. (2015). The spatial distribution of shallow-water (<150 m) black corals (Cnidaria:
875 Antipatharia) in the Hawaiian Archipelago. *Marine Biodiversity Records*, 8.
876 <https://doi.org/10.1017/S1755267215000202>

877 Wagner, D., Luck, D. G., & Toonen, R. J. (2012). The Biology and Ecology of Black Corals (Cnidaria:
878 Anthozoa: Hexacorallia: Antipatharia). In *Advances in Marine Biology* (Vol. 63, pp. 67–132).
879 Elsevier. <https://doi.org/10.1016/B978-0-12-394282-1.00002-8>

880 Warner, G. F. (1981). *Species Descriptions and Ecological Observations of Black Corals (Antipatharia)*
881 *from Trinidad*. 17.

882 Yao, C.-L., & Somero, G. N. (2014). The impact of ocean warming on marine organisms. *Chinese*
883 *Science Bulletin*, 59(5–6), 468–479. <https://doi.org/10.1007/s11434-014-0113-0>

884 Yesson, C., Bedford, F., Rogers, A. D., & Taylor, M. L. (2017). The global distribution of deep-water
885 Antipatharia habitat. *Deep Sea Research Part II: Topical Studies in Oceanography*, 145, 79–86.
886 <https://doi.org/10.1016/j.dsr2.2015.12.004>

887

888